Composites Science and Technology 71 (2011) 1427–1434

Contents lists available at ScienceDirect

Composites Science and Technology

journal homepage: www.elsevier.com/locate/compscitech

Surface coating of multi-walled carbon nanotube nanopaper on shape-memory polymer for multifunctionalization

Haibao Lu [a,b], Yanju Liu [c], Jihua (Jan) Gou [b,*], Jinsong Leng [a,*], Shanyi Du [a]

[a] Center for Composite Materials and Structures, Harbin Institute of Technology, Harbin 150001, China
[b] Department of Mechanical, Materials and Aerospace Engineering, University of Central Florida, Orlando, 32816 FL, USA
[c] Department of Aerospace Science and Mechanics, Harbin Institute of Technology, Harbin 150001, China

ARTICLE INFO

Article history:
Received 14 December 2010
Accepted 20 May 2011
Available online 31 May 2011

Keywords:
A. Carbon nanotubes
A. Nano composites
B. Electrical properties
B. Surface treatments

ABSTRACT

We are presenting a method of synthesizing three-dimensional self-assembled multi-walled carbon nanotube (MWCNT) nanopaper on hydrophilic polycarbonate membrane. The process is based on the very well-defined dispersion of nanotube and controlled pressure vacuum deposition procedure. The morphology and structure of the nanopaper are characterized with scanning electronic microscopy (SEM) over a wide range of scale sizes. A continuous and compact network observed from the microscopic images indicates that the MWCNT nanopaper could have highly conductive property. As a consequence, the sensing properties of conductive MWCNT nanopaper are characterized by functions of temperature and water content. Meanwhile, in combination with shape-memory polymer (SMP), the conductive MWCNT nanopaper facilitates the actuation in SMP nanocomposite induced by electrically resistive heating. Furthermore, the actuating capability of SMP nanocomposite is utilized to drive up a 5-gram mass from 0 to 30 mm in height.

1. Introduction

As a promising material in nanoscience and nanotechnology, one dimensional nanoscale materials such as carbon nanotube (CNT), attracting significant interest for its superior mechanical and electrical characteristics. Both theoretical and experimental results have shown that CNTs have a high elastic modulus in the range of 500–600 GPa [1]. The estimated maximum tensile strength of CNTs is close to 200 GPa [2], which is 40 times higher than carbon fiber [3]. Molecular dynamic simulations revealed that thermal conductivity of CNTs could be as high as 6600 W/mK at room temperature [4]. It has been prospected that CNTs are among the most promising reinforcement materials or functional agents for developing high performance multifunctional nanocomposites [5,6]. Single-walled carbon nanotube (SWCNT) and multi-walled carbon nanotube (MWCNT) both can carry a current density of as high as 1×10^9 amp/cm^2 [7–9], while only 1×10^6 amp/cm^2 for copper wire [10]. CNTs also shows great flexibility compared with conventional fiber reinforcements [11,12]. Since CNTs are considered by many researchers as the most promising reinforcement material for high performance structural and multifunctional composites [6,13], strong interests exist in developing CNT-reinforced nanocomposites [14,15].

Traditionally, researchers fabricated composites by directly mixing the CNTs into polymers and made the final composites. However, CNTs have a strong tendency to form bundles and aggregate together because of their high surface area and the strong van der Waals interaction [16]. Their very stable chemical characteristics and lack of functional sites on the surface make efficiently dispersing CNTs into polymer matrix and controlling the final nanostructure of the nanocomposites during the processing difficult, particularly for high CNT loading nanocomposites. An *in situ* polymerization method is used to effectively disperse CNTs into resin matrix with an aid of sonication. Besides the dispersion issue, the rapidly increasing viscosity of the mixture made high CNT loading in nanocomposites difficult here. Their practical application, however, poses a great challenge to nanotechnology due to their nanoscale size. A good solution to the problem seems to be using them in the forms of CNTs in the macroscopic level, such as forests, yarns and films. A recent idea to address these problems involves initially making a macroscopic paper-like CNT films, also called nanopapers, are self-supporting networks of entangled CNT in a random fashion and held together by van der Waals interactions at the tube–tube junctions [17]. The potential applications of nanopapers and their enabled nanocomposites are promising and huge, including fire protection [18], lightning strike protection (with an unusually high current-carrying capability) and electromagnetic shielding interference [19]. An in-depth understanding of the key factors controlling the effectiveness of CNT nanopaper for sensing capability and multifunction is indispensable.

* Corresponding authors. Tel./fax: +86 451 86402328 (J. Leng).
E-mail addresses: jihua.gou@ucf.edu (J. Gou), lengjs@hit.edu.cn (J. Leng).

0266-3538/$ - see front matter Crown Copyright © 2011 Published by Elsevier Ltd. All rights reserved.
doi:10.1016/j.compscitech.2011.05.016

Shape-memory polymers (SMPs) are attracting attention of scientists and technologists alike as an exciting class of smart materials that can transform from one shape into another in response to external stimuli such as heat, light, electric, or magnetic field [20–22]. SMP has a capability of memorizing its permanent shape. They can be manipulated and "fixed" to a temporary shape under specific conditions of temperature and stress, and subsequently relax to the original, stress-free state in presence of an external stimulus. Many studies have featured various materials based on chemically or physically cross-linked polymer systems, each attempting to extend their application range and revealing structure property relationships [23,24]. Most of the current research in the field of SMPs is focused on the intrinsic function of the shape-memory effect, including efficient fixing of a temporary shape, recovery to an equilibrium shape, and the exploitation of different stimuli as triggers. We herein describe a SMP nanocomposite in which a conductive capability provides additional functionality in electrically resistive heating by incorporating with CNT nanopaper. Furthermore, the CNT nanopaper is integrated into a styrene-based SMP with sensing and actuating capabilities. The CNT nanopaper is expected to transform insulating SMP into conducing. The electrical property of nanopaper and its enabled SMP nanocomposite is determined by a four-point probe method. As a consequence, the sensing properties of nanopaper are characterized by functions of temperature and water content. These two experimental results both aid the use of SMP nanocomposites as sensors that respond to the changes in temperature or humidity. At the same time, the actuating capability of SMP nanocomposites is also validated and demonstrated. The dynamic mechanical analysis result first reveals the output strength of SMP nanocomposites in the shape recovery process. The actuating capability of SMP nanocomposites is subsequently created from the shape-memory effect of SMP. This function is conducted by electrically resistive heating and simultaneously is utilized to drive up a 5-gram mass from 0 to 30 mm in height.

2. Experimental details

The MWCNT employed in this work is supplied by Shenzhen Nanometer Gang Co., Ltd., China. The nanotubes are synthesized by chemical vapor deposition (CVD) and have a purity of around 95%. The diameter ranges between 10 and 20 nm and length of 1–15 μm. The MWCNTs were first dispersed into water with the aid of Triton X-100 surfactant ($C_{14}H_{22}O(C_2H_4O)_n$, the molecular structure contains a hydrophilic polyethylene oxide group and hydrocarbon lipophilic (or hydrophobic) group). The hydrophobic group of surfactant backbone is close contact with the MWCNT, resulting in the modified MWCNT having a hydrophilic polyethylene oxide group. Therefore, the modified MWCNT will be well-dispersed into the water. The MWCNT suspension was sonicated with a high-intensity sonicator (MISONIX Sonicator 4000, Qsonica, LLC, Newtown, Connecticut, USA) at room temperature for 30 min. After the initial 15 min sonication, both MWCNT suspension and probe were cooled back to room temperature. The sonication was carried out again for another 15 min under the same condition. The MWCNT suspension was then filtrated through a 0.4 μm (the diameter of gap) hydrophilic polycarbonate membrane (HTTP Isopore™ membrane filter with a diameter of 142 mm) under a positive pressure of 100–120 psi to separate the MWCNTs from the solvent and form a MWCNT nanopaper. After the filtration, the MWCNT nanopaper was dried in a heating oven at 120 °C for 2 h to further remove the remaining water and surfactant. Nanopapers with preformed tube networks have a macroscale dimension and can be handled as conventional fiber mats to attain controllable reinforcement dispersion and volume content, as shown in the Fig. 1. The dried nanopaper showed a dimensional shrinkage of 64.8% (from 142 mm to 92 mm in diameter). The Veriflex®S, VF 62 SMP (supplied from Cornerstone Research Group Inc., Dayton, Ohio, USA) is a styrene-based matrix and polymerized with the curing agent (dibenzoyl peroxide harder) at a weight ratio of 24:1. A resin transfer molding process was used for molding and curing. The nanopaper was placed on the bottom of the mold. The SMP matrix was then injected into the mold. After the mold filling, the mixture was cured with a ramp of approximately 1 °C/min from room temperature to 75 °C. The sample was then held at 75 °C for 3 h before being ramped to 90 °C at 15 °C/180 min. Finally, it was ramped to 110 °C at 20 °C/120 min to produce the final nanocomposites. Nanocomposites with preformed tube networks and various MWCNTs loading (1.47%, 3.10%, 4.95% and 7.02% by weight) were manufactured.

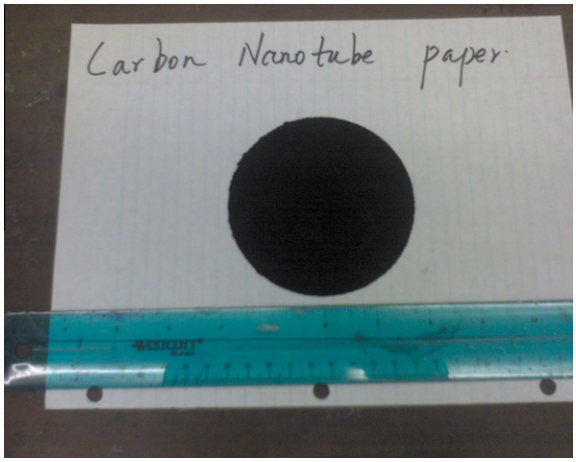

Fig. 1. The MWCNTs self-assemble on hydrophilic polycarbonate membrane to form the nanopaper with a diameter of 92 mm.

3. Results and discussion

3.1. Morphology and structure of MWCNT nanopaper

The morphology and network structure of MWCNT nanopaper were characterized by scanning electron microscope (SEM) (ZIESS Ultra-55) at 10 kV. Fig. 2a and b are typical surface views of raw MWCNT arrays about 100 nm and 1 μm, respectively. As shown in Fig. 2a, there is no large particle that came from the aggregates can be found, owing to MWCNTs being well dispersed in the suspension. Fig. 2b evidenced an individual MWCNT with a diameter of 10–20 nm, and length of 1–15 μm. It is observed the multi-scale porous structure of nanopaper, and the porous structure with average pore size of 50–1000 nm. Based on the SEM observation, it is found that individual nanotube gather together to form bundles (ropes) through van der Waals forces. They are mostly arranged in ropes or bundles with close-packed stacking. And a network structure is formed by molecular interaction and mechanical interlocking among nanotubes. Such a continuous network will act as a conductive path for electrons, making the nanopaper and its enabled nanocomposite electrically conductive.

3.2. Electrical resistivity measurement

The electrical resistivity of the MWCNT nanopapers and their SMP nanocomposites was determined by a four-point probe apparatus (SIGNATONE QUADPRO system), which is mainly incorporated of a Keithley resistivity tester and a Keithley picoammeter/voltage source. The apparatus has four probes in a straight line with an equal interprobe spacing of 1.56 mm. The radius of the

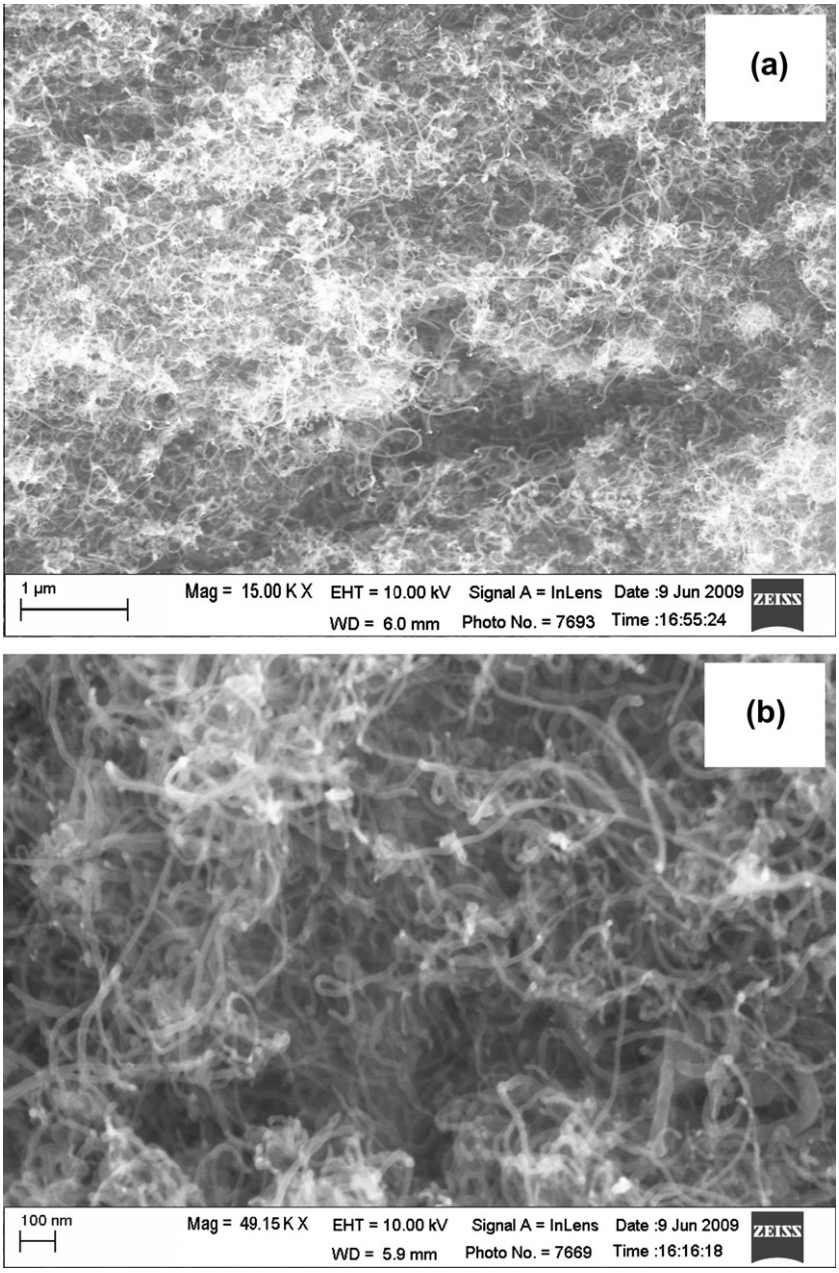

Fig. 2. Morphology and network structure of MWCNT nanopaper. (a) At a scale of 1 μm and (b) at a scale of 100 nm.

probe needle is 100 μm. A constant current was passed through the two outer probes and an output voltage was measured across the inner probes with the voltmeter. The characteristic electrical resistivity of the nanopapers and nanocomposites, from different zones, as a function of weight concentration of MWCNT nanopaper measured at room temperature was plotted and figured out in Fig. 3. Five zones on the surface of samples were chosen to determine the uniformity in electrical property of tested sample. And the average value of five times measurement was used to characterize the electrical resistivity. In the following study, all the electrical resistivity values are determined in this manner. Each data point denotes the resistivity of a zone. In all four nanopapers and their nanocomposites, there are differences in resistivity among zones as well as among samples. This is indicative of the appreciable variability in nanopaper concentration and nanocomposite. With an increase in weight concentration of nanopaper from 0.6 to 2.4 g, the average electrical resistivity of corresponding nanopaper and nanocomposite is decreased from 4.8904 to 0.9354 ohm cm, and 8.953 to 0.8348 ohm cm, respectively.

As is observed from the microstructure of nanopaper, the electrical property is determined by the continuously conductive network. When more conductive individuals are involved into the network, many more conductive paths are formed in the continuous network. Given more conductive paths in one bulk, more electrons are involved in electrical circuit owing to the cross section area proportionally increased. Therefore, the electrical current amplitude and current-carrying capability increases because more electrons are forced to pass through the cross section of the bulk. Furthermore, more paths in conductive network could yield a short distance for electrons flow. The velocity of cyclic electrons flow in electrical circuit is significantly accelerated. On the other hand, with density of nanopaper increase, the pore size in nanopaper

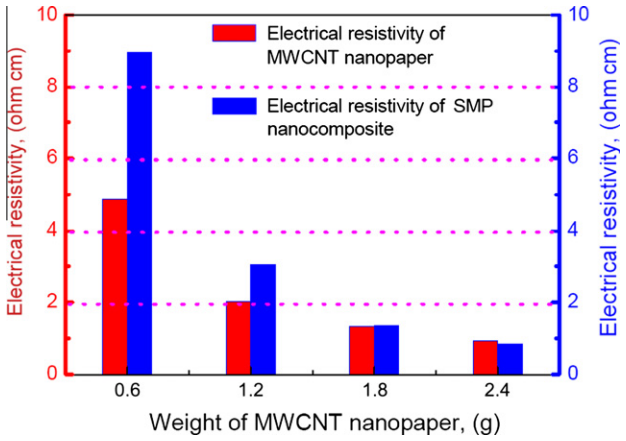

Fig. 3. Comparison of electrical resistivity of MWCNT nanopapers and their enabled SMP nanocomposites with varying weight concentration of nanotubes.

structure will get smaller. These three factors would make electrical resistivity of nanopaper bulk therefore lowered, based on the Eq. (1). In summary, as more nanotubes involved into conductive network, the electrical resistivity of nanopapers and their enabled nanocomposites is therefore be lowered.

$$I = neSv \tag{1}$$

where n is the number of charge per unit volume, e is the charge of a electron, S is the cross-section area of the conductor, and v is the velocity of the electron.

Moreover, the evolution change in electrical resistivity of MWCNT nanopapers and their enabled SMP nanocomposites is compared as function of weight concentration of MWCNT. The resistivity of SMP nanocomposites with respectively 0.6 g, 1.2 g and 1.8 g MWCNT nanopaper is higher than that of the corresponding nanopaper. While the resistivity of SMP nanocomposite with 2.4 g MWCNT nanopaper is lower than that of the corresponding nanopaper. Therefore, the interaction between polymer and nanopaper could be considered to account for it. As is observed from microscopic structure, the nanopaper bulk is a pore mass. In the fabrication, polymer resin would penetrate into or through the nanopaper, occupies the pore locations in nanopaper structure and make dispersion of MWCNTs rearranged. When the pore locations are occupied by polymer, the density of nanopaper is altered due to that the bonding of an amount of MWCNTs is changed from van der Waals force to chemical bonding provided from polymer. And as the density of nanopaper is influenced by chemical bonding, the dispersion of MWCNTs in nanopaper is also be rearranged. The electrical conductive paths and network are then reset, making the electrical resistivity of nanopaper therefore changed. As the nanopaper with a relative low weight concentration of MWCNT, the pore fraction in nanopaper structure is high, owing to its low density. When the pore locations are occupied by the insulating polymer, the continuously conductive network would be destroyed or obstructed. Here, the electrical resistivity of composites becomes more obviously high in comparison with corresponding neat nanopaper. While the nanopaper with a high weight concentration, the pore fraction in nanopaper structure will become small, owing to its relative high density. Here, by incorporating with polymer resin, the polymer could not destroy or obstruct continuously conductive network. In contrary, the polymer would make conductive network structure of nanopaper more concentrated, due to that chemical bonding provided by polymer tends to support a stronger interaction among MWCNTs compared with initial van der Waals bonding. Here, the electrical resistivity of nanocomposites is lower than the neat nanopaper. However, this change would be slight, owing to this interaction only occurs in a small domain. Otherwise it would destroy the conductive network and plays a negative role in influencing the electrical property of nanopaper.

3.3. Response of nanopaper sensor to temperature

Normally, the temperature range in a practical engineering application of MWCNT nanopaper and their nanocomposites are ranged from room temperature to 100 °C. Thus, the dependence of electrical resistivity on temperature in this range should be considered. The dependence of electrical resistivity on temperature was determined by measuring the electrical resistivity while heating the specimens to a desired temperature.

Positive temperature coefficient (PTC) effect and negative temperature coefficient (NTC) effect in conductive materials have been an area of active research since the initial observation of the phenomenon [25]. Alternative, these integrate materials with sensing capability to response ambient temperature change. NTC effect is characterized by the restoration of electrical conductivity upon further heating the specimens. It is thought to be related to the electrons mobility with temperature increase [26]. In this study, thermal effect of conductive MWCNT nanopaper was determined from the electrical resistivity dependent temperature experiment. Nanopapers with different weight concentration of 0.6, 1.2, 1.8 and 2.4 g MWCNTs were used. Fig. 4 shows the evolution change in electrical resistivity of four nanopapers as their temperatures increased from room temperature to 120 °C. As presented from these curves, all four nanopapers possess a characteristic NTC behavior, where the electrical resistivity value is decreased with increasing ambient temperature. Taking for an example, the initial and final values of electrical resistivity for 2.4 g MWCNT nanopaper are 0.9354 Ω cm (at room temperature) and 0.4989 Ω cm (at 120 °C), respectively. This NTC effect of these conductive nanopapers could be attributed to the following fact, as the sample being heated to a higher temperature, electrons in conductive network pick up energy and electrons flow becomes accelerated. The velocity of cyclic electrons flow in electrical circuit will be herein accelerated, resulting in the period of cyclic electrons flow shortened. This approach would therefore make electrical resistivity of bulk lowered.

In comparison of these four curves, it is found that the electrical resistivity of MWCNT nanopaper with 0.6 g weight concentration shows the most great depression with temperature increase. As details, the electrical resistivity of 0.6 g MWCNT nanopaper decreases from 4.8904 to 3.6671 (1.2233) ohm cm with temperature increased from room temperature to 120 °C, while the electrical resistivity of 2.4 g MWCNT nanopaper decreases from 0.9354 to

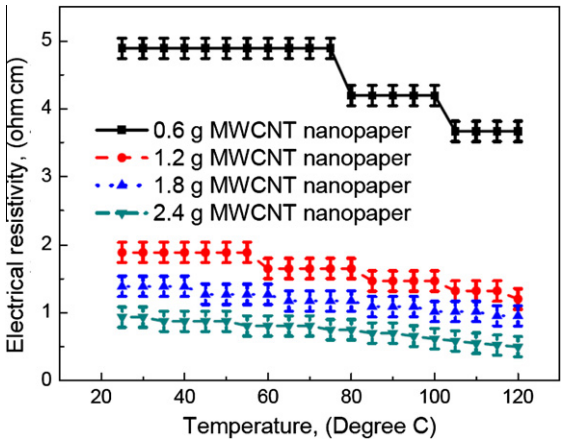

Fig. 4. Values of electrical resistivity versus temperature for the MWCNT nanopaper.

0.4989 (0.4365) ohm cm. This phenomenon also results from electrons movement in the electrical circuit. As is known, with temperature increase, the micro-Brownian motion of individual MWCNT will become more significance. And Brownian motion is closely related to the university of normal distribution and belongs to a continuous stochastic process. Therefore, in the nanopaper with more weight concentration of MWCNT, there are many more nanotubes involved to prevent or postpone the beamed electrons motion in the electrical circuit. As a result, the electrical current in nanopaper with lower weight concentration will have a more obvious NTC effect. Because beamed electrons motion is influenced by the Brownian motion of relative a fewer amount of MWCNTs. In summary, these two factors synergistically influence the electrical property of nanopaper in response to temperature.

3.4. Nanopaper sensor for detecting variation in water content

With an unusually high current-carrying capability, the potential applications of nanopapers and nanocomposites are promising and huge, such as fire protection [18] and lightning strike protection [19]. As a porous structure, the ability to detect water content inside a water-permeable nanopaper is also important for fire protection. Thunder and lightning sometimes is corporate with raining in nature. Therefore, study on the synergistic effect of electrical property and water content on the properties of nanopaper will become prominent. After being dried in a vacuum oven at 100 °C for 1 h, the nanopapers with various weight concentrations of MWCNTs were used. First, nanopapers absorbed 300% their respective weights of distilled water. Then nanopaper/water systems were dried in vacuum oven at 120 °C for different durations, from 0 to 30 min at a interval of 2.5 min. Then, the weight of nanopaper and electrical resistivity were measured, respectively. Based on the change in weight of the nanopaper, we therefore calculate the quality of evaporated moisture and the weight ratio between water to nanopaper as follows:

$$R = \frac{W_0 + 300\% \times W_0 - W_1}{W_0} \quad (2)$$

where W_0 is the neat weight of nanopaper sample, $300\% \times W_0$ is the weight of water content, W_1 is the weight of nanopaper/water system after various drying times in vacuum oven. Fig. 5a shows the weight ratio between water to nanopaper as a function of 2.5 min of drying time.

Fig. 5b shows the evolution change in electrical resistivity of the MWCNT nanopapers as the water content in the samples went from 300% of the weight of the respective samples to approximately 0%. From the figure, it can be seen that four samples, when containing 300% of their respective weights in water, exhibits relatively high values of resistivity, i.e. 1.873 ohm cm for the 0.6 g MWCNT nanopaper, 3.517 ohm cm for the 1.2 g MWCNT nanopaper, 6.918 ohm cm for the 1.8 g MWCNT nanopaper, and 9.663 ohm cm for the 2.4 g MWCNT nanopaper. And the general evolution of the resistivity decreased as the water content in the samples decreased. After drying the nanopapers for 2.5 min in heating oven at 120 °C, it can be seen that the resistivity for all the nanopaper samples significantly dropped. From this point, the nanopapers show a slight increase in electrical resistivity and then begin to level off. However, the sample containing 2.4 g MWCNT continues to decrease in resistivity up until 15 min of drying time and then shows a slow rise in resistivity before leveling off. At the 15 min mark, when the electrical resistivity reached to its lowest value for the 2.4 g MWCNTs sample, it contained 10.4% of its weight in water. One possible explanation for the lowest values of resistivity occurring when each sample still contained a significant amount of water is the condition in which H_2O molecules within the MWCNT sample matrix behave like electron donors as

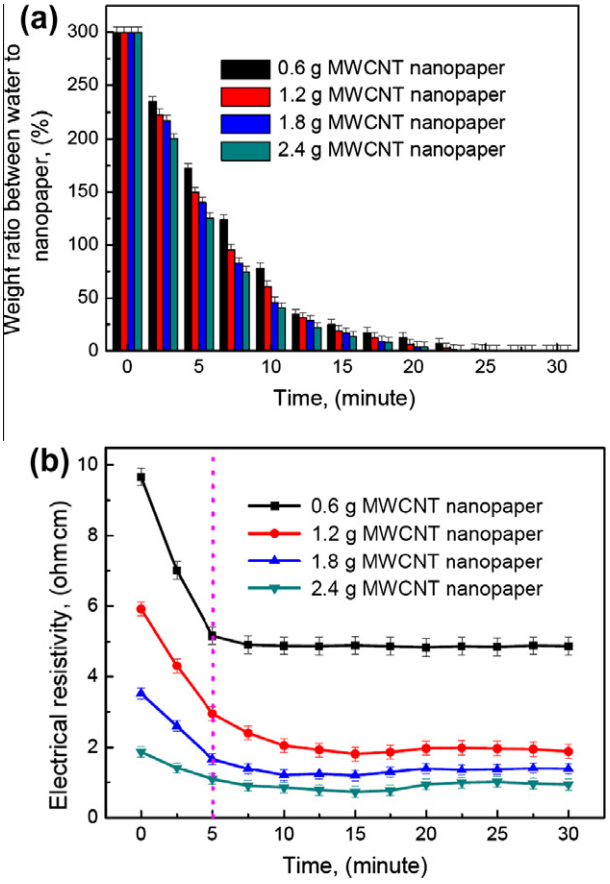

Fig. 5. (a) Values of weight ratio between water to nanopaper versus drying time and (b) values of electrical resistivity versus drying time for the MWCNT nanopaper.

in the case of a p-type semiconductor [27]. On the other hand, as the dielectric constant of MWCNT is ranged from 1.5 to 5, while that of water is 80 at 25 °C. The dielectric constant of water is always higher than that of MWCNT. Thus, with high water content, the dielectric constant of nanopaper/water system is proportionally high, resulting in the electrical properties of system altered.

3.5. Actuating capability of nanopaper enabled SMP nanocomposite by electricity

In the following section, the actuating properties of the conducting SMP/nanopaper nanocomposite are studied by introducing a parameter called recovery strength, which shows the stress generated per unit of strain. To determine the recovery strength, dynamic mechanical analyzer (TA Instruments Q800 DMA) test was carried out to measure the storage modulus and loss modulus of the nanocomposite as function of temperature. All experiments were performed on the single cantilever mode at an oscillation frequency of 1.0 Hz, a constant heating rate of 10 °C/min, and temperature range from −20 to 160 °C. In the DMA measurement of nanocomposites with various weight fractions of MWCNT nanopaper, the storage modulus, loss modulus and tangent delta were recorded with respect to temperature. The storage modulus is the modulus of the elastic portion of the material, while the loss modulus is the modulus of the viscous portion. The tangent delta, defined as the ratio of the loss modulus over the storage modulus, indicates the damping capability of a material. In addition, the peak of tangent delta curve is defined as the glass transition temperature (Tg) of polymeric materials, as shown in Fig. 6a.

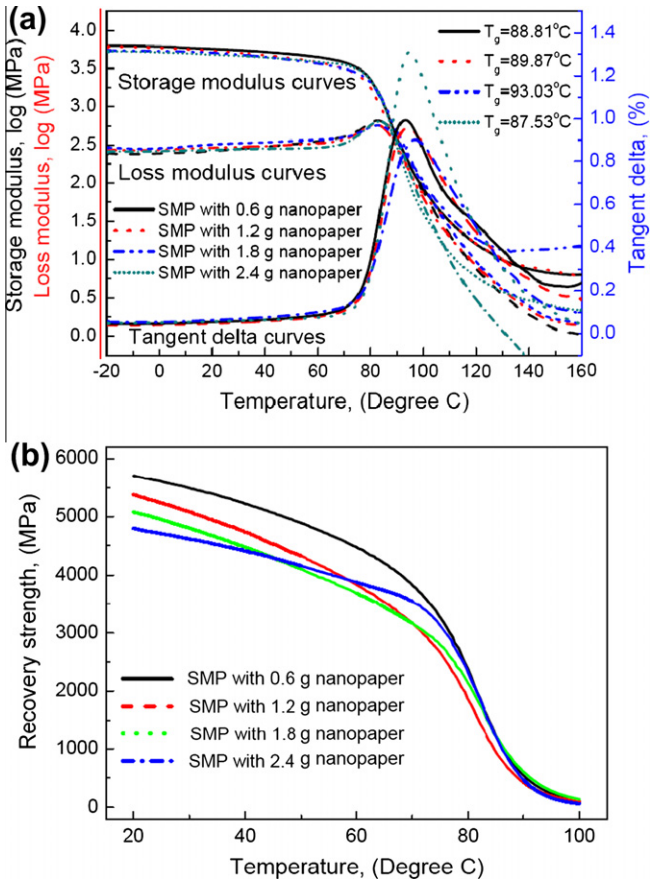

Fig. 6. (a) Storage modulus, loss modulus and tangent delta curves, and (b) recovery strength of SMP nanocomposites with different weight concentration of MWCNT nanopaper.

The proposed recovery strength of the SMP nanocomposite incorporated with MWCNTs nanopaper can be expressed as follows:

$$E = \sqrt{E_s^2 + E_l^2} \tag{3}$$

where E represents the shape recovery strength (normally elastic modulus), E_s is the storage modulus and E_l is the loss modulus. After calculation, curves of recovery strength as function of temperature are plotted. Four specimens that respectively cut from 0.6 g MWCNT nanopaper, 1.2 g MWCNT nanopaper, 1.8 g MWCNT nanopaper, and 2.4 g MWCNT nanopaper enabled SMP nanocomposite are adopted for comparison. It is presumed that the SMP nanocomposites show their shape recovery performance within the temperature range of 20–100 °C.

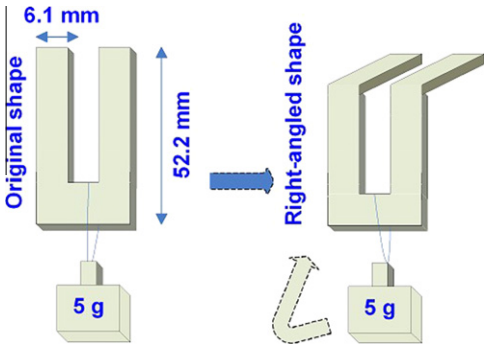

Fig. 8. Schematic illustration of the setup for the actuating capability test of nanocomposite.

As shown in Fig. 6b, for each sample, the recovery strength decreases slowly at first, and then a sharp decrease is observed around 60 °C. Because the storage of elastic strain energy in polymer network is not released when the temperature is relatively low, and the shape-memory effect cannot be fully expressed at this state. Therefore, the elastic modulus is relatively high and more stress will be generated per unit of strain. In other words, if the material is fixed and exposed to external forces, more resistance stress will be generated inside the material. However, with an increase in temperature, the molecular chains in polymer network get enough energy to separate and the locomotory units start to move, resulting in the decrease in elastic modulus and elastic strain energy released. Here, we will see the shape recovery of SMP nanocomposite. Even though the nanocomposite start to show its shape-memory effect around its *Tg*, the polymer transfers from glassy state to rubbery state, and the recovery strength decreases drastically since the material begin to show viscoelasticity. Moreover, with shape-memory effect of SMP, the nanopaper enabled SMP nanocomposite shows more potential for the design and manufacture of smart actuators, which can be controlled by the electrical current other than the direct heating approach.

First, we would like to demonstrate the electrically resistive heating-driven shape-memory effect of SMP nanocomposite. Then, this exciting nanocomposite will be utilized as smart actuator. Fig. 7 shows the recovery of SMP nanocomposite from a fixed bent shape to its flat permanent shape under a constant DC voltage. To minimize the mechanical constraint imposed by the electrodes, the

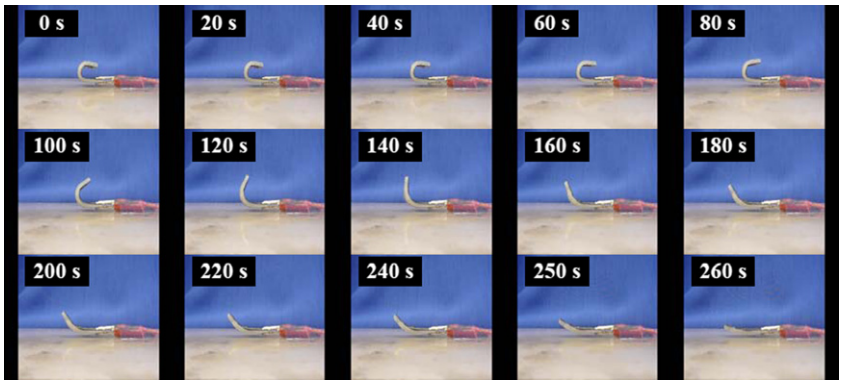

Fig. 7. Series of photographs showing the macroscopic shape-memory effect of SMP composite integrated with 1.8 g MWCNT nanopaper. The permanent shape is a flat strip of composite material, and the temporary shape is deformed as right-angled shape.

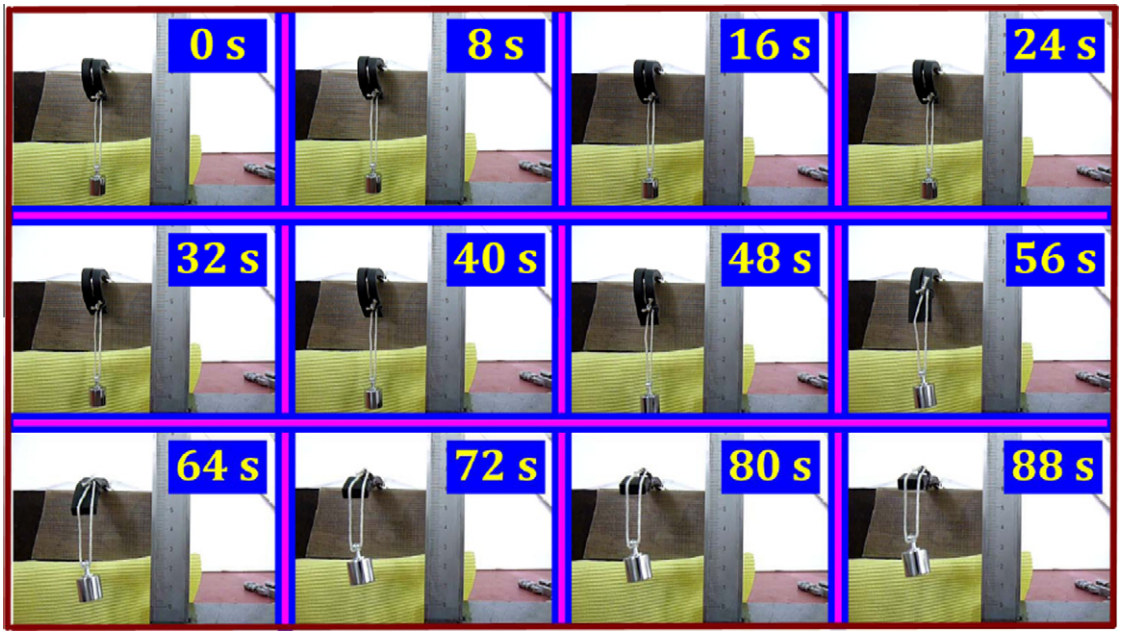

Fig. 9. Series of photographs showing the electro-activate shape memory effect of SMP/nanopaper nanocomposite and actuating the motion of 5-gram mass. The permanent shape is a plane stripe of nanocomposite and the temporary shape is deformed as a right-angled shape.

shape recovery was conduct under a relatively unconstrained condition. Experimentally, the recovery process was characterized using a bending test method [26]. The flat (permanent shape) nanocomposite sample with a dimension of 120 mm × 10 mm × 6 mm was bent as "U"-like shape (temporary shape) at 85 °C, where the *Tg* of pure polystyrene SMP is approximate 62 °C. This shape was kept until the specimen was cooled down to room temperature. No apparent shape recovery was found after the deformed specimen being kept in air for 2 h, until a constant 8.4 V DC voltage was applied to the SMP nanocomposite sample. The nanocomposite took 260 s to complete the shape recovery from the temporary shape to its permanent shape. Initially the SMP sample showed a little recovery ratio during the first 60 s. It then started to exhibit a faster recovery behavior until 260 s.

In combination of the excellent electrical properties and shape-memory effect, electrically resistive heating-driven shape recovery of SMP/nanopaper nanocomposite (cut from 2.4 g MWCNT nanopaper enabled nanocomposite) has been demonstrated and is used actuate the motion of a 0.5 g weight simultaneously recorded with a video camera. The used nanocomposite, which is incorporated of 25 vol.% MWCNT nanopaper, is about 115.6 mm × 6.1 mm × 2.4 mm. The flat (permanent shape) nanocomposite was first bent as right-angled shape (temporary shape) at 100 °C, where its *Tg* is approximate 87.53 °C (as shown in Fig. 6a). This shape was kept until the nanocomposite was cooled down to room temperature. No apparent shape recovery was found after the deformed specimen being kept in air for 2 h. Fig. 8 is a schematic illustration of the setup for the actuating capability test of nanocomposite.

The shape transition of SMP nanocomposite in a DC field of 35 V is documented with a digital camera. In 88 s, the starting conversion of the flexural shape is observed to be completed. As shown in Fig. 9, initially the nanocomposite showed a little recovery ratio during the first 7 s. It then started to exhibit a faster recovery behavior until 80 s. The final shape is close to the original flat shape. And the 5-gram mass is driven up from 0 to 30 mm in height. It should be noted that the rate of shape recovery is strongly dependent on the magnitude of the applied voltage and the electrical resistivity of the composite.

4. Concluding remarks

This paper presents a systematic study of the morphology, nano-sized structure, temperature and water content dependent electrical properties, as well as electro-activated shape-memory behavior of SMP/nanopaper nanocomposites. These basic investigations integrate nanocomposite with sensing and actuating capabilities. Main conclusions to be drawn as follows: (1) Owing to the inherent conductive properties of MWCNT, the scale-up MWCNT nanopaper has an excellent electrical property and electrical current carrying capability, resulting in the potential applications of MWCNT nanopaper are promising and huge. This present study is expected to make tremendous process in the development of nanopaper as sensors. (2) In combination of electrically conductive MWCNT nanopaper and the shape-memory effect of SMP, the developed SMP nanocomposites are integrated with sensing and actuating capabilities. MWCNT nanopaper sensor has been explored for detecting variation in temperature and water content. Meanwhile the nanopaper facilitates the electrically resistive heating transfer to the underlying SMP. In parallel with sensing capabilities of nanopaper, the developed nanocomposites also have an actuating capability by integrating with recovery strength in the recovery process of SMP. Smart devices and structures utilizing this exciting nanocomposite are currently being designed in our lab. We envision great potential of this nanocomposite in applications encompassing actuators, sensors morphing skin and deployable structures.

Acknowledgments

This work has been financially supported by "the Fundamental Research Funds for the Central University (Grant No. HIT. NSRIF. 201157)".

References

[1] Pipes RB, Frankland SJV, Hubert P, Saether E. Self-consistent properties of the carbon nanotubes and hexagonal arrays as composite reinforcements. Compos Sci Technol 2003;63(10):1349–58.

[2] Yu MF, Files BS, Arepalli S, Ruoff RS. Tensile loading of ropes of single wall carbon nanotubes and their mechanical properties. Phys Rev Lett 2000;84(24):5552–5.
[3] Dekker C. Carbon nanotubes as molecular quantum wires. Phys Today 1999;52(5):22–8.
[4] Berber S, Kwon YK, Tomanek D. Unusually high thermal conductivity of carbon nanotubes. Phys Rev Lett 2000;84:4613–6.
[5] Thostenson ET, Ren ZF, Chou TW. Advances in the science and technology of carbon nanotubes and their composites: a review. Compos Sci Technol 2001;61(13):1899–912.
[6] Lau KT, Hui D. The revolutionary creation of new advanced materials-carbon nanotube composites. Compos Part B: Eng 2002;33(4):263–77.
[7] Yao Z, Kane CL, Dekker C. High-field electrical transport in single-wall carbon nanotubes. Phys Rev Lett 2000;84(13):2941–4.
[8] Lu HB, Yu K, Liu YJ, Leng JS. Sensing and actuating capabilities of shape memory polymer composite integrated with hybrid filler. Smart Mater Struct 2010;19:065014.
[9] Lee YH, Lee JH, Chung SJ, Lee S, Ju BK. Carrier carrying capacity of one-step grown suspended carbon nanotube bridge with carbon nanotube contact electrodes: for practical one-dimensional electronics. Appl Phys Lett 2006;89:073109.
[10] Li CY, Thostenson ET, Chou TW. Effect of nanotube waviness on the electrical conductivity of carbon nanotube-based composites. Compos Sci Technol 2008;68(6):1445–52.
[11] Leng JS, Lu HB, Liu YJ, Huang WM, Du SY. Shape-memory polymers – a class of novel smart materials. MRS Bull 2009;34(11):848–55.
[12] Iijima S, Brabec C, Maiti A, Bernholc J. Structural flexibility of carbon nanotubes. J Chem Phys 1996;104(5):2089–92.
[13] Lu HB, Liu YJ, Gou J, Leng JS, Du SY. Synergistic effect of carbon nanofiber and carbon nanopaper on shape memory polymer composite. Appl Phys Lett 2010;96:084102.
[14] Biercuk MJ, Llaguno MC, Radosavljevic M, Hyun JK, Johnson AT, Fischer JE. Carbon nanotube composites for thermal management. Appl Phys Lett 2002;80:2767.
[15] Schadler LS, Giannaris SC, Ajayan PM. Load transfer in carbon nanotube epoxy composites. Appl Phys Lett 1998;73:3842.
[16] Wang Z, Liang ZY, Wang B, Zhang C, Kramer L. Processing and property investigation of single-walled carbon nanotube (SWNT) buckypaper/epoxy resin matrix nanocomposites. Compos Part A – Appl Sci Manuf 2004;35(10):1225–32.
[17] Lu HB, Liu YJ, Gou J, Leng JS, Du SY. Electrical properties and shape-memory behavior of self-assembled carbon nanofiber nanopaper incorporated with shape-memory polymer. Smart Mater 2010;19:075021.
[18] Zhao Z, Gou J. Improved fire retardancy of thermoset composite modified with carbon nanofibers. Sci Technol Adv Mater 2009;10:015005.
[19] Gou J. Single-walled nanotube bucky paper and nanocomposites. Polym Int 2006;55:1283–8.
[20] Lu HB, Yu K, Sun SH, Liu YJ, Leng JS. Mechanical and shape-memory behavior of shape-memory polymer composites with hybrid fillers. Polym Int 2010;59(6):766–71.
[21] Mather PT, Luo XF, Rousseau IA. Shape memory polymer research. Annu Rev Mater Res 2009;39:445–71.
[22] Lu HB, Liu YJ, Leng JS, Du SY. Qualitative separation of the effect of solubility parameter on the recovery behavior of shape-memory polymer. Smart Mater Struct 2009;18:085003.
[23] Leng JS, Lv HB, Liu YJ, Du SY. Electroactivate shape-memory polymer filled with nanocarbon particles and short carbon fibers. Appl Phys Lett 2007;91:144105.
[24] Leng JS, Lv HB, Liu YJ, Du SY. Synergic effect of carbon black and short carbon fiber on shape memory polymer actuation by electricity. J Appl Phys 2008;104:104917.
[25] Zhang CS, Ni QQ, Fu SY, Kurashiki K. Electromagnetic interference shielding effect of nanocomposites with carbon nanotube and shape memory polymer. Compos Sci Technol 2007;67(14):2973–80.
[26] Luo Y, Wang G, Zhang B, Zhang Z. The influence of crystalline and aggregate structure on PTC characteristic of conductive polyethylene/carbon black composite. Eur Polym J 1998;34:1221–7.
[27] Zahab A, Spina L, Poncharal P. Water-vapor effect on the electrical conductivity of a single-walled carbon nanotube mat. Phys Rev B 2000;62(15):10000–3.